Available online at www.sciencedirect.com
SCIENCE DIRECT®
Journal of Nuclear Materials 334 (2004) 40–46
journal of nuclear materials
www.elsevier.com/locate/jnucmat

Breakaway bubble growth during the annealing of helium bubbles in metals

J.H. Evans *

27 Clevelands, Abingdon, Oxon OX14 2EQ, UK
EURATOM/UKAEA Fusion Association, Culham Science Centre, Oxfordshire OX14 3DB, UK

Received 26 January 2004; accepted 22 April 2004

Abstract

Recent experimental studies on the annealing of helium implanted copper showed unusual surface pinholes which could not be explained using conventional bubble migration and coalescence theory. However, computer simulation results indicated that at some threshold, breakaway bubble swelling was taking place, thus giving a plausible picture of the experimental results. In the present study the computer simulations have been repeated for an initially uniform helium level in bulk material, allowing the threshold effects to be examined without any surface effects and any loss of helium. Assuming equilibrium bubble conditions, the results showed that when bubble coarsening reached an average of 20% swelling, breakaway swelling occurred. This phenomenon has been examined as a function of helium content and results extrapolated (with some assumptions) to other temperatures and metals. The implications for fusion reactor materials is briefly discussed.

1. Introduction

A recent experimental study by Escobar Galindo et al. [1] in which copper was implanted with helium ions to give a peak helium level of less than 2% at 130 nm from the surface, produced the surprising result that after annealing at 973 K, ~80% of the helium was released and surface pinholes seen, even though the average bubble size predicted from migration and coalescence theory was ~14 nm. The appearance of the pinholes and their size were consistent with scanning electron microscopy images of subsurface bubbles (radius ~150 nm) found after surface removal using electropolishing. In computer simulations [2] of random bubble migration and coalescence, an unexpected phenomenon was found in which at sufficient values of local swelling, super-large bubbles were formed centred at the helium peak which grew quickly to bisect the surface, thus providing a probable explanation for the surface pinhole observations and the large subsurface bubbles. Furthermore the magnitude of the gas release fitted the experimental data extremely well.

The appearance of particularly large bubbles during annealing of bubble populations are also found in the earlier work of Birtcher [3] on helium implanted nickel and seem to be consistent with the Escobar Galindo et al. results.

In the light of these experimental and computer simulation studies, it was felt that further insight into the breakaway growth of bubbles might be gained by simulation of gas bubble annealing in a bulk situation, thus avoiding any complication due to initial non-uniform helium concentrations or to bubble loss at surfaces. This would allow the fundamental rules controlling the formation of the large bubbles (probably at some critical swelling, but possibly at some other bubble concentration–radius combination) to be found, and the rapid increase in bulk swelling to be studied. This breakaway

* Tel./fax: +44-1235 525059.
E-mail address: jhevans@lineone.net (J.H. Evans).

0022-3115/$ - see front matter © 2004 Elsevier B.V. All rights reserved.
doi:10.1016/j.jnucmat.2004.04.349

swelling phenomenon also deserves investigation in relation to its possible application to bulk materials containing high helium levels that might be found in fusion reactor environments. Although the basic results presented here are for different levels of helium in copper annealed at 973 K, assumptions on the surface diffusivity allow extrapolation to other temperatures, and more tentatively to other metals.

2. Outline of modelling

Brief details will be given here; a fuller description of the methodology is given in Appendix A. In the main computer program an initial population of 4000 bubbles was set up in a pseudo-random distribution within a $(100\ \text{nm})^3$ block, equivalent to a bubble density of $4\times10^{18}/\text{cm}^3$. The distribution was made following a procedure suggested by Foreman [4], with every new bubble position being tested against all previous bubble coordinates to ensure that initially a minimum distance existed between bubbles. The starting radius was chosen to reflect the helium level being studied. To prevent too much quantization of bubble radii after coalescence, the starting radii were treated to give a Gaussian distribution of radii about the average. In the simulation of the high temperature anneal, the modelling simulated the random walk of bubbles, allowing the migration and coalescence of the bubbles to be followed under thermal equilibrium conditions. Spherical equilibrium bubbles were assumed, with coalesced bubbles immediately re-equilibrating to a new radius to maintain the usual $P = 2\gamma/r$ relation where P is the bubble pressure, r its radius and γ the surface energy. Calculations were simplified by using the ideal gas law to relate the bubble sizes with their helium content.

The model allowed individual bubbles to move randomly according to surface diffusion kinetics given by the appropriate equation for bubble diffusion, D_b, [5,6]

$$D_b = (3\Omega^{4/3})/(2\pi r^4)D_s, \tag{1}$$

where Ω is atomic volume of the matrix and D_s the surface diffusivity, is given by

$$D_s = D_o \exp(-E_s/kT), \tag{2}$$

where E_s is the activation energy for surface diffusion. Using random walk theory, it is easy to show that for a bubble with radius r_i, the jumpstep in a given time is proportional to $1/r_i^2$. After each jumpstep cycle in which all bubbles were moved, bubbles were tested against their near neighbours for touching, and if so were allowed to coalesce, to give a new bubble with a radius reflecting its new larger helium content. Because of the inverse relation of bubble pressure with radius, any coalescence under equilibrium bubble conditions leads, as is well known, to an increase in the vacancy to helium atom ratio and hence an increase in local swelling. Bubbles were also tested in position against the block surfaces. If they crossed the surface, they were introduced on the opposite face to maintain periodic boundary conditions. The overall procedure allowed the bubble size parameters and swelling to be followed with time.

One problem with modelling coalescence events is that the process leads to a reduction in bubble numbers and therefore in statistics. In a recent simulation of Ostwald ripening (for voids in silicon [7]), an analogous problem was treated by using a cloning procedure. In the present case, after the bubble numbers were reduced by a factor of eight from 4000 to 500, the block was cloned and used to create a new block with volume a factor of eight greater, thus returning to 4000 bubbles in the system but maintaining the radius distributions. While the local spatial distributions of bubbles within the eight subblocks were initially identical, their subsequent random movement quickly introduced differences. This iteration procedure could be repeated as many times as required.

The swelling value in the work was always defined (arbitrarily) as the bubble volume divided by the original volume. Since these values reached 20% and greater, it was felt important to make the simulation more realistic by uniformly increasing the block size at regular intervals by an appropriate amount to reflect the swelling. At the same time all the bubble positions were changed, again appropriately, moving slightly apart but keeping their relative positions within the block.

3. Results

In this work the initial calculations were made using parameters for copper at 973 K as used in the near-surface calculations of Ref. [2]. The important parameter of surface diffusivity was taken from the work of Willertz and Shewman [8] who give an average value of $8\times10^{-9}\ \text{cm}^2/\text{s}$ at 973 K. Uniform helium contents of 1.0, 2.0 and 3.0 at.% helium have been studied with several computer runs being made at each concentration. As will be seen, although there were run to run quantitative variations, the main qualitative result of breakaway swelling was exactly as found in the simulation of results for implanted helium. The results also show the effect of varying the helium concentration and also discuss the extrapolation of the basic results to other temperatures and to other metals.

3.1. Breakaway bubble formation

During the first part of the anneals, the bubble coarsening behaviour was much as expected with a

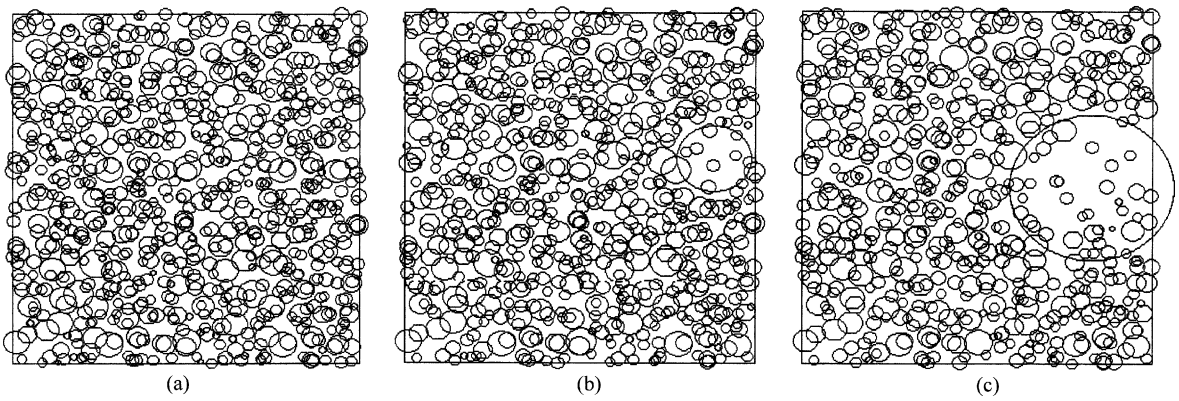

Fig. 1. Projection through the working volume showing the formation and growth of a large bubble; (a) time = 27.9 s, (b) time = 33.5 s, (c) time = 38.9 s. The projected area has sides of 424 nm.

gradual coarsening of the bubble populations, the rise in average radius closely following the expected $t^{1/5}$ variation with time [9,10]. In this region all runs gave results which were quantitatively extremely close. However, eventually, out of what appeared to be a typical distribution of bubbles, a large bubble was formed. Although, as shown later, there were clear variations between computer runs for the annealing time required to form these large bubbles, the qualitative picture was always the same. An example, showing the emergence of a large bubble for a 3% helium level, is seen in Fig. 1 simulation results. Unlike the near surface simulations in Ref. [2] where bubble growth stopped when the surface was touched, in the bulk case there was no physical restriction to bubble growth.

The formation of the large bubbles was very strongly reflected in the bubble size and swelling parameters, as seen in Fig. 2 for the 2% helium case. The smooth rise in all these parameters with annealing time was interrupted by the very clear sharp rises in the swelling (with the breakaway swelling occurring when the average swelling reached close to 20%) and in the value of the root mean cube radius. Only a small perturbation in the average radius line was apparent. Another way of demonstrating the breakaway effect was in a plot of the volume of the largest bubble compared to the value of the average bubble. As shown in Fig. 3, this ratio changes over a relatively short period from a steady state value (of around 20) to a value well in excess of 1000. However, once a large bubble has formed, the simulations might be expected to be affected more and more by the assumptions such as the immediate return to thermal equilibrium after coalescence.

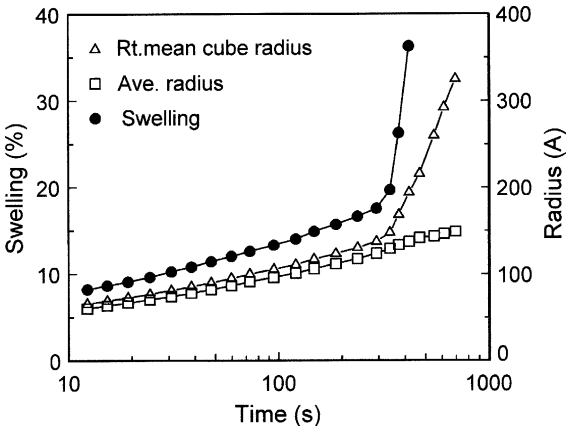

Fig. 2. Typical results, here for 2 at.% He, showing the sharp breakaway in the swelling and root mean cube radius coincident with the formation of large bubbles.

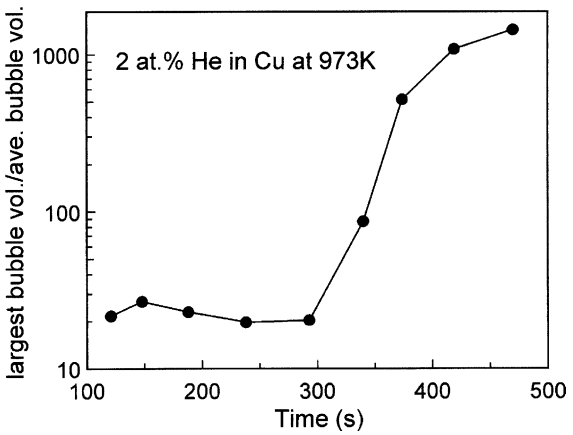

Fig. 3. Graph showing the rapid rise in ratio of largest bubble volume to the average bubble volume during the growth of a breakaway bubble.

3.2. Statistics

As already mentioned, up to the breakaway point the bubble parameters were very consistent from run to run.

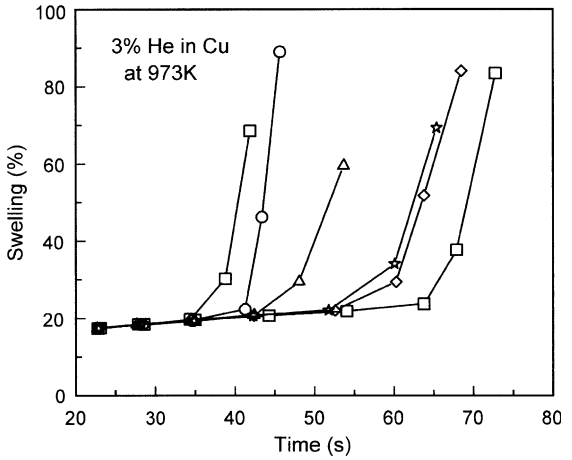

Fig. 4. Bubble swelling as a function of time for 3% He in copper at 973 K showing the run to run variations for the breakaway swelling.

However, the time at which the breakaway occur varied considerably, as might be expected from the accumulated randomness imposed on the bubble movements in the relatively small simulation volume. This is demonstrated for the 3% helium case in Fig. 4. The variation seen here, of between about 35 and 65 min was surprisingly large, but the same order of variation, almost a factor of 2, was also found for the 1% and 2% helium levels.

3.3. Influence of helium content

The effect of varying the helium concentration made no obvious difference to the breakaway swelling phenomenon except in the time required for the breakaway swelling to occur. This is seen in Fig. 5 where representative data for three helium levels are shown. The important result from this figure is that is shows the initiation of breakaway effects occurs in all cases when the average swelling reaches approximately 20%. For the three helium levels studied (1%, 2%, and 3%), the approximate average times for this breakaway were 3×10^4, 400 and 50 s, respectively.

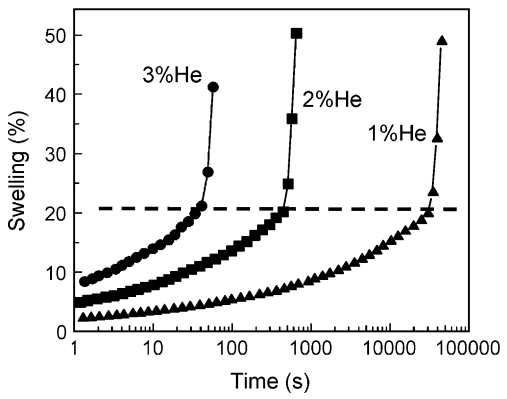

Fig. 5. Effect of helium level on time to breakaway swelling. The horizontal dashed line emphasises the 20% swelling level.

3.4. Extrapolation to other temperatures

In Appendix A it is shown that the time increments for a given set of starting conditions (i.e. given helium content) are proportional to $[(9\Omega^{4/3}/\pi)D_s]^{-1}$; the same must hold for the total sum of the increments, i.e. the total time. Thus using Eq. (1) for D_s we can write the breakaway time, t_b, as

$$t_b = K(x\%)\exp(+E_s/kT), \tag{3}$$

where $K(x\%)$ is a constant for a given $x\%$ helium concentration.

The data at 973 K for copper can thus be translated to any temperature provided the assumptions in the model still hold, and we have a value for the surface diffusion energy. Although data for the surface diffusion obtained from bubble behaviour as a function of temperature is shown in Ref. [8], the error bars are too large to allow the surface diffusion energy to be obtained with any confidence. An alternative approach is to take the 973 K value of 8×10^{-9} cm^2/s already used from this work for the surface diffusivity and combine it with a calculated value for the pre-exponential, D_o thereby allowing a value for E_s to be deduced. We can write $D_o = \nu\lambda^2/6$ where ν is the jump frequency, usually assumed to be 10^{13}/s, and λ is the jumpstep, i.e. lp/$\sqrt{2}$, with lp being the lattice parameter. For copper, we obtain $D_o = 1.1\times10^{-3}$ cm^2/s, and thus applying Eq. (2) at 973 K obtain a value of $E_s = 1.0$ eV. Although this value is not inconsistent with the data in Ref. [8], the approximations of ideal gas and the instantaneous growth of coalesced bubbles back to equilibrium would anyway make extrapolation somewhat approximate. Nevertheless, the approach seems worthwhile if only to get an order of magnitude feel for possible effects. Proceeding on this basis, the K values required for Eq. (3) are trivially obtained from the breakaway times already given and are: $K(1\%) = 0.194$; $K(2\%) = 2.56\times10^{-3}$: $K(3\%) = 3.23\times10^{-4}$. With these values it was straightforward to obtain the breakaway time for different helium contents as a function of anneal temperature. The results are shown in Fig. 6.

For copper half the melting point is at 405 °C. Below this temperature one might expect that the assumption of instantaneous re-equilibration of coalesced bubbles holds less strongly. However, it is worth noting that Johnson and Mazey [11] in discussing some in situ recordings of helium bubble behaviour in implanted copper during hot stage annealing, reported clear bubble coalescence as low as 325 °C ($0.44T_m$).

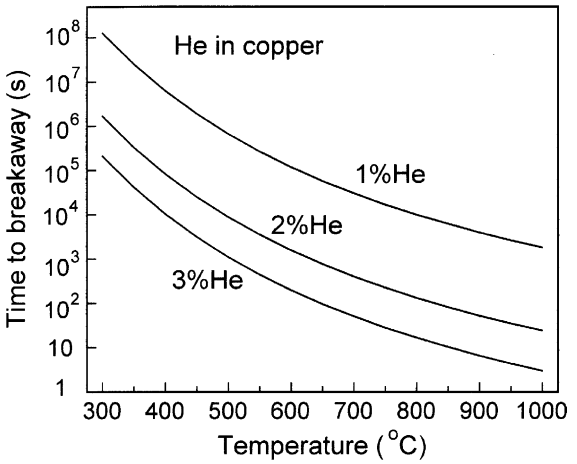

Fig. 6. The extrapolation of the computed results for helium in copper at 973 K to other temperatures.

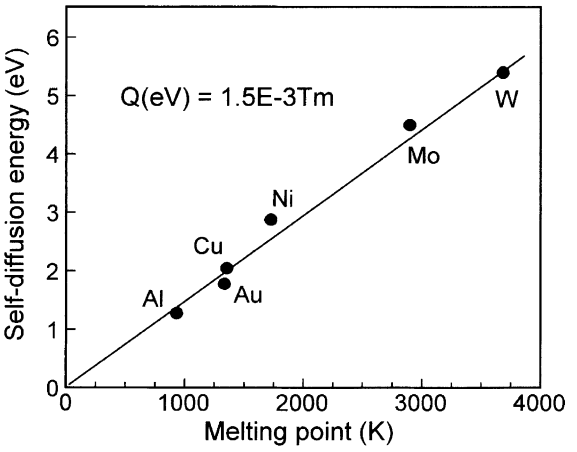

Fig. 7. Self-diffusion energies for different metals as a function of melting temperature, T_m [10].

3.5. Extrapolation to other metals

The extrapolation difficulties of the previous section also apply here but again in the sense of giving a guideline, it seems a worthwhile exercise to extend the model to other metals. To do this requires an expression for self-diffusion energy in terms of metal melting point. Such an expression has been proposed by Neumann and Neumann [12] based on surface measurements. They suggested that for $T/T_m < 0.75$, the value of D_s could be expressed as

$$D_s = 1.4 \times 10^{-2} \exp(-5.64 \times 10^{-4} T_m/kT) \text{ cm}^2/\text{s}. \quad (4)$$

However, for bubble applications this expression gives values which are several orders of magnitude too large to fit experimental data. This has been pointed out in bubble diffusion papers on copper and gold [8,13]. A possible explanation lies in the suggestion of Mikhlin that in the high pressure bubble environment surface diffusion can be much reduced [14].

Because of the difficulties in using Eq. (4), it is proposed here to use an alternative approach. It turns out that for copper, the activation energy for surface diffusion deduced in Section 3.3 is approximately half the self-diffusion energy. If for the sake of argument this is assumed for other metals, extrapolation of the copper results to other metals is relatively straightforward since one can obtain results in terms of T/T_m where T_m is the melting temperature. It is not difficult or novel to suggest a relation between activation energies and melting temperature. In Fig. 7 this is done for the self-diffusion energy using data from Siegel [15].

It can be seen that the relation $Q = 1.5 \times 10^{-3} \cdot T_m$ eV is a reasonable fit to Fig. 7 data. If, we assume the value of E_s is given by $E_s = Q/2$, then $E_s = 7.5 \times 10^{-4} \cdot T_m$. Replacing the value of E_s in Eq. (3) we obtain:

$$t_b = K(x\%) \exp(7.5 \times 10^{-4} \cdot T_m/kT), \quad (5)$$

This expression allow us to use the values of K obtained from copper to plot a universal curve, Fig. 8, for different metals showing the breakaway time as a function of T/T_m. The approach uses the approximation that the pre-exponential in Eq. (2) is invariant with metal so that in practice when other assumptions are also considered, Fig. 8 can only be an order of magnitude guide to the importance of the breakaway swelling. Nevertheless this could still be useful. As modelled in this paper, the results would apply to situations where materials containing helium are then subjected to high temperature annealing.

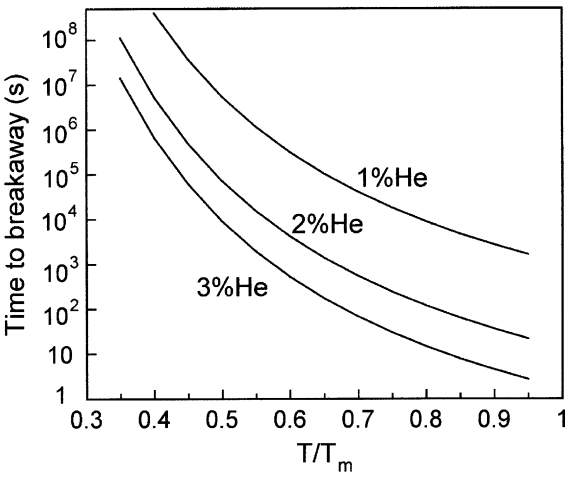

Fig. 8. Universal plot of time to breakaway as a function of T/T_m, see text.

4. Discussion

This paper has extended recent work on breakaway swelling during the annealing of near surface helium bubbles to the case of bubble swelling in bulk material, under initial conditions of a uniform helium level. During the computer simulation of bubble movement, and the consequent bubble coalescence, a breakaway swelling effect is again seen. The simulations suggested that the effect is initiated when the average swelling reaches ~20% after which the overall swelling increases sharply to high levels.

The phenomenon of breakaway swelling has been discussed previously by Barnes [16]. By considering equations for bubble movement under driving forces he derived a condition that bubble touching would be inevitable at zero bubble velocity when the swelling reached 33%. However, the equations for random walk bubble coalescence used in Refs. [9,10] to give the average bubble radius as a function of time, temperature, gas concentration, etc. do not lead to any breakaway condition. These equations do not involve bubble size distributions. The breakaway swelling in the present simulations appears to develop as follows. There will always be a largest bubble as referred to in Section 3.1 where its volume in relation to the average bubble volume is discussed. Translating this result to radius, the largest radius will be about 2.7 times the average. At some stage, this largest bubble reaches a value where, as it grows, its surface area increase provides an increasingly larger sink for the local smaller bubbles which are more mobile. As shown in Fig. 1 this breakaway condition is not instantaneous but clearly it is fast. There is no intuitive reason for the critical 20% swelling threshold but the simulation results were very consistent.

Although any results in practice will be modified by the assumptions in the model, particularly the supply of thermal vacancies (and possible spatial effects [17]), the qualitative effects should remain. This could be important in predicting the behaviour of helium in materials under fusion reactor conditions although the effect could be limited by grain boundaries and gas release. Nevertheless, for worse case scenarios, the results of Fig. 8 would suggest that even material with low helium levels could give high swellings if held at moderate temperatures for long times or inadvertently (e.g. under accident conditions) at high temperatures for short times.

Acknowledgements

This work was jointly funded by the United Kingdom Engineering and Physical Sciences Research Council and by EURATOM. The author thanks Dr Sergei Dudarev and Dr Ian Cook for their interest in this work. The author also thanks Dr Ramon Escobar Galindo for discussions and acknowledges his deep debt to the late Dr Tom van Veen for his help on this and many other papers in the field of inert gas behaviour in metals.

Appendix A

In this section we give a more formal description of the methodology used in the simulation program. In each cycle the bubbles (having a wide distribution of radii) perform one jump in a random direction, at which stage each bubble is tested against its nearest neighbours for touching, and thus whether coalescence should take place. The main question is how one chooses a time-step appropriate to the scale of the bubble distribution and diffusion parameters.

It is worth starting by introducing the main diffusion equation for bubbles, radii r, moving under surface diffusion conditions

$$D_b(r) = (3/2\pi) \cdot (\Omega^{4/3}/r^4).D_s, \tag{A.1}$$

where Ω is the atomic volume of the metal and D_s is the surface diffusion coefficient.

If the jumpstep cycle takes place in a time dt then the distance l moved in this time by a bubble of radius r will be

$$l(r) = \sqrt{(6D_b \cdot dt)}. \tag{A.2}$$

Combining Eqs. (A.1) and (A.2) we obtain

$$l(r) = [((9/\pi)\Omega^{4/3}D_s dt)^{1/2}]/r^2 \tag{A.3}$$

or

$$l(r) = \mathrm{jsp}/r^2, \tag{A.4}$$

where jsp is a jumpstep parameter given by $\mathrm{jsp} = [((9/\pi)\Omega^{4/3}D_s dt)^{1/2}]$.

While this is useful, it is also necessary to connect the time step to the scale of the bubble system. A measure of the system scale, ss, was chosen to be related to the bubble density, rho, and the average radius, r_{ave} by the relation

$$\mathrm{ss} = (\mathrm{rho})^{-1/3} - 2 \cdot r_{ave}. \tag{A.5}$$

It can be seen that this is roughly the average distance between bubble surfaces.

Reference has been made to the nearest neighbours of the bubbles in testing for touching. Each bubble in fact had a neighbourhood list giving the bubbles which lay within a distance ss; this list was revised every 100 cycles. The purpose of the list was of course to avoid the considerable computing time required if every bubble was to be tested for touching against every other bubble in each cycle. It was decided that the time step could be

defined to ensure that the smallest bubble in the system (i.e. the fastest moving) should not diffuse more than the value of ss in the 100 cycles between the neighbourhood list revision. This in turn ensured that only the bubbles on the neighbourhood list of a given bubble could reach the bubble in the 100 jumps; thus potential collisions between bubbles would not be missed.

Random walk theory shows that in a given number of cycles, N, only a very small fraction of random walkers travel further than three times the root mean square value, i.e. $3j\sqrt{N}$, where j is the jumpstep. If this distance is reasonably described as the maximum distance moved, then for the smallest bubble, radius r_{sml} we can equate its maximum movement, j_{sml} in 100 cycles to the value of the average bubble spacing, bs. Thus

$$\mathrm{bs} = 3j_{\mathrm{sml}} \cdot 10, \quad \text{i.e.} \quad \mathrm{bs} = 30j_{\mathrm{sml}}. \tag{A.6}$$

From Eq. (A.4) we have $j_{\mathrm{sml}} = \mathrm{jsp}/r_{\mathrm{sml}}^2$ and hence we can write

$$\mathrm{jsp} = r_{\mathrm{sml}}^2 \mathrm{bs}/30. \tag{A.7}$$

Since we already have an expression for jsp in terms of dt it is easy to rearrange the equations to obtain the relation

$$\mathrm{d}t = \mathrm{jsp}^2/((9/\pi)\Omega^{4/3}D_{\mathrm{s}}). \tag{A.8}$$

Clearly from Eqs. (A.7) and (A.8) the value of dt can be computed continuously throughout the program in terms of r_{sml} and bs, thus reflecting the scale of the bubble distribution and the fastest moving bubble. Results using these equations were compared with data obtained with a value of 60 instead of 30 in Eq. (A.7), giving time increments a factor of 4 smaller. No differences were perceived in the data up to the formation of the breakaway bubbles. However, their subsequent growth appeared to be faster with the smaller time step.

References

[1] R. Escobar Galindo, A. van Veen, J.H. Evans, H. Schut, J.Th.M. de Hosson, Nucl. Instrum. and Meth. B 217 (2004) 262.
[2] J.H. Evans, R. Escobar Galindo, A. van Veen, Nucl. Instrum. and Meth. B 217 (2004) 276.
[3] R.C. Birtcher, in: S.E. Donnelly, J.H. Evans (Eds.), Fundamental Aspects of Inert Gases in Solids, Plenum, New York, 1991, p. 133.
[4] A.J.E. Foreman, unpublished work 1998.
[5] R. Kelly, Phys. Stat. Solidi 21 (1967) 451.
[6] F.A. Nichols, J. Nucl. Mater. 30 (1969) 143.
[7] J.H. Evans, Nucl. Instrum. and Meth. B 196 (2002) 125.
[8] L.E. Willertz, P.G. Shewmon, Metall. Trans. 1 (1970) 2217.
[9] E.E. Gruber, J. Appl. Phys. 38 (1967) 243.
[10] P.J. Goodhew, S.K. Tyler, Proc. Roy. Soc. A 377 (1981) 151.
[11] P.B. Johnson, D.J. Mazey, Radiat. Eff. 53 (1980) 195.
[12] G. Neumann, G.M. Neumann, in: Surface self-diffusion of metals, Diffusion Monograph Series, Diffusion Information Centre, Ohio, 1972.
[13] J.H. Evans, A. van Veen, J. Nucl. Mater. 168 (1989) 12.
[14] E.Ya. Mikhlin, Phys. Stat. Solidi (a) 56 (1979) 763.
[15] R.W. Siegel, in: J. Takamura, M. Doyama, M. Kiritani (Eds.), Proceedings of the International Conference on 'Point defects and defect interactions in metals' Yamada, 1981, University of Toyko, 1983, p. 533.
[16] R.S. Barnes, J. Nucl. Mater. 11 (1964) 135.
[17] J.H. Evans, A. van Veen, J. Nucl. Mater. 233–237 (1996) 1179.